

Low-resistance, high-force, and large-ROM fabric-based soft elbow exosuits with adaptive mechanism and composite bellows

HUANG WeiCheng^{1,2†}, FENG Miao^{1,2†}, YANG DeZhi^{1,2} & GU GuoYing^{1,2,3*}

¹ Robotics Institute, School of Mechanical Engineering, Shanghai Jiao Tong University, Shanghai 200240, China;

² State Key Laboratory of Mechanical System and Vibration, Shanghai Jiao Tong University, Shanghai 200240, China;

³ Meta Robotics Institute, Shanghai Jiao Tong University, Shanghai 200240, China

Received July 17, 2022; accepted October 14, 2022; published online December 26, 2022

Due to the lightweight and compliance, fabric-based pneumatic exosuits are promising in the assistance and rehabilitation of elbow impairments. However, existing elbow exosuits generally suffer from remarkable mechanical resistance on the flexion of the elbow, thus limiting the output force, range of motion (ROM), and comfortability. To address these challenges, we develop a fabric-based soft elbow exosuit with an adaptive mechanism and composite bellows in this work. With the elbow kinesiology considered, the adaptive mechanism is fabricated by sewing the interface of the exosuit into spring-like triangle pleats, following the profile of the elbow to elongate or contract when the elbow flexes or extends. The composite bellows are implemented by further sealing a single blade of bellows into two branches to enhance the output force. Based on these structural features, we characterize the mechanical performance of different soft elbow exosuits: exosuit with normal bellows-NB, exosuit with adaptive mechanism and normal bellows-AMNB, exosuit with adaptive mechanism and composite bellows-AMCB. Experimental results demonstrate that by comparing with NB, the mechanical resistance of AMNB and AMCB decreases by 80.6% and 78.6%, respectively; on the other hand, the output torque of AMNB and AMCB increases to 120.3% and 207.0%, respectively, at 50 kPa when the joint angle is 120°. By wearing these exosuits on a wooden arm model (1.25 kg), we further verify that AMCB can cover a full ROM of 0°–130° at the elbow with 500 g weight. Finally, the application on a health volunteer with AMCB shows that when the volunteer flexes the elbow to lift a weight of 500 g, the sEMG activity of the biceps and triceps is markedly reduced.

wearable robots, rehabilitation robots, soft robot applications, soft actuators design

Citation: Huang W C, Feng M, Yang D Z, et al. Low-resistance, high-force, and large-ROM fabric-based soft elbow exosuits with adaptive mechanism and composite bellows. Sci China Tech Sci, 2022, 65, <https://doi.org/10.1007/s11431-022-2233-3>

1 Introduction

Elbow plays an important role in activities of daily living (ADLs), such as feeding, writing, and lifting. Nevertheless, the functionalities of the elbow are likely to be damaged by stroke, arthritis, parkinsonism, etc. For example, there are over 12 million new stroke patients around the world per year, and up to 50% of them would suffer from an upper-

extremity impairment, involving elbow impairment, which makes them unable to flex their elbows actively or lift heavy loads [1–3]. Although physical rehabilitation has been widely used for elbow treatment, the treatment course of physical rehabilitation is repetitive, usually lasts for a long time, and requires the assistance of professional therapists, which is not affordable for many patients [4,5].

Alternatively, a variety of wearable robotic devices have been developed for the assistance and rehabilitation of elbow impairment. Among them, rigid wearable devices are the most developed, such as MIT-Manus, ARMin, and CADEN-

†These authors contributed equally to this work.

*Corresponding author (email: guguoying@sjtu.edu.cn)

7 [6–8]. Rigid wearable devices perform fast response and high output force. However, their rigid frames and components bring about problems of poor portability, complex linkages, substantial inertia, and even joint misalignment [9,10].

Compared with rigid wearable devices, soft wearable devices (i.e., exosuits), such as electromechanical cable-driven exosuits [11–13] and pneumatic soft exosuits [14–16], are more lightweight to wear, easier to fabricate, and safer for human-robot interaction [17]. Cable-driven exosuits mostly use Bowden cables and soft harnesses to pull the arm and convert the pulling force into joint torque. For example, Cappello et al. [11] used two series of elastic elements in the cable pulley system and a soft fabric frame to provide compliant elbow motion assistance. Lessard et al. [13] developed a bio-inspired exosuit by arranging the cable along the primary muscles responsible for elbow assistance. However, cable-driven exosuits have problems like uncomfortable joint compression and skin friction, and they usually require precise placement of anchor points or additional rigid parts to generate enough joint torque [18–20].

Pneumatic soft exosuits are commonly fabricated by elastomers or fibers with inherent compliance. For instance, Noritsugu et al. [14] assembled a wearable exoskeleton by the sandwiched curved artificial muscle, which comprises rubber tubes and nylon bands, achieving safe and smooth elbow flexion assistance. Gao et al. [15] fabricated an elastomer-based bending actuator by silicone casting with sensors embedded. Based on the actuator, they present a pneumatic soft elbow exosuit to assist the aging population. Nevertheless, these elastomer-based actuators or exosuits typically exhibit a low stiffness-to-weight ratio, limiting the output force of exosuits.

As an emerging technology, fabric-based pneumatic soft exosuits are even more lightweight, wear-resistant, mechanically transparent, and easier to integrate [21,22]. These exosuits produce output force generally through actuators with specialized structural design [23–28]. For example, a fabric inflatable beam arranged along the elbow provides an output force of 16.5 N at 80 kPa to assist elbow extension [23]. Bellows-shaped exosuit, comprising an array of TPU chambers sheathed by Nylon fabric, can produce a torque of 27.6 N m at 300 kPa to assist the elbow in lifting motion [25]. The exosuit with antagonistic soft actuators fabricated by TPU-coated nylon fabric is able to generate 5 N m torque at 100 kPa and cover 54.7° of the elbow flexion ROM [26].

Despite many efforts in designing fabric-based pneumatic soft exosuits, there is remarkable mechanical resistance due to a mismatch of motion between the elbow and exosuit. Improving the output force and the range of motion (ROM) remains challenging for enhanced capability in practical applications [23,25–27]. In this work, we consider the kinesiology of the elbow and present a low-resistance, high-

force, and large-ROM fabric-based pneumatic soft elbow exosuit with an adaptive mechanism and composite bellows.

Design, fabrication, characterization, and applications are organized to verify the exosuits. The main contributions are summarized as follows. (1) By employing the kinesiology of the elbow, we propose an adaptive mechanism that makes the exosuit flexibly elongate or contracts like a spring when the elbow flexes or extends, which reduces the mechanical resistance of the elbow exosuit by 78.6%. (2) We introduce composite bellows to reinforce the actuator stiffness for higher output torque. Experimental results show that compared to the exosuit with normal bellows (NB), our exosuit improves the output torque to 207.0% under typical conditions. (3) Experiments on a wooden arm model demonstrate that our exosuit can cover a full ROM of 0°–130° at the elbow [29]. Further verification on a health volunteer shows that the sEMG activity of people's biceps and triceps during lifting is markedly reduced with our exosuit. (4) We integrate a soft wearable system controlled via the smartphone, including the exosuit and the control panel (Figure 1), of which the exosuit weighs only 344.2 g and the whole system weighs 1302.7 g.

2 Design of soft wearable elbow exosuit

2.1 Elbow kinesiology

The elbow of a human mainly comprises the humerus and the ulna (Figure 2(a)). The joint flexion is a compound motion of rolling and sliding [29], which causes the profile elongation of the elbow determined by

$$\Delta L = \left(W + \frac{\delta}{2} \right) \theta_{\text{joint}}, \quad (1)$$

where ΔL , W , δ , and θ_{joint} represent the profile elongation of



Figure 1 (Color online) Overview of the low-resistance, high-force, and large-ROM fabric-based soft elbow exosuit with adaptive mechanism and composite bellows. (a) The elbow exosuit is wearable and portable; (b) the system can be remotely controlled by a smartphone; (c) the elbow exosuit.

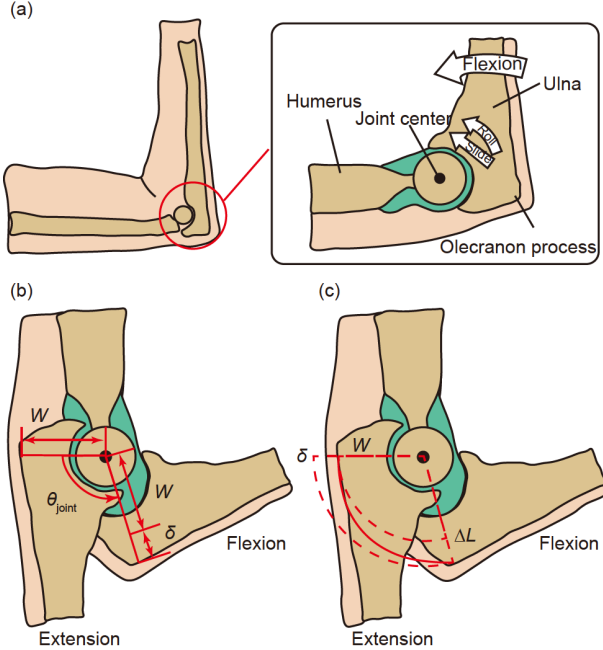


Figure 2 (Color online) Kinesiology of the elbow. (a) The sagittal section view through the humero-ulnar joint during elbow flexion; (b) the parameters related to elbow profile elongation; (c) the trajectory of the olecranon process and estimation of the elbow profile elongation.

the elbow, the distance between the joint center and the olecranon process when the elbow fully extends, the translation offset caused by the sliding of the ulna, and the flexion angle of the joint, respectively (Figure 2(b)). Here, the spiral-shaped profile elongation in Figure 2(c) is approximately obtained by taking the average of two extreme distances W and $W+\delta$. The motion mismatch between exosuit and elbow can lead to remarkable mechanical resistance and limit the output force and ROM.

2.2 Design

The exosuit with adaptive mechanism and composite bellows (AMCB) is mainly composed of 4 layers of textiles (Figure 3(a), see Supporting Information Movie S1). Firstly, the structural feature, composite bellows, is achieved by folding and partially sealing the top layer-① into an array of blades with two branches ("Y" shape). Then, the top layer-① is attached to the bottom layer-③ to form an airtight chamber. To prevent air binding, an air spacer-② is inserted between these two layers of textiles (Figure 3(a) I and II). Next, the bottom of the composite bellows is corrugated into triangle pleats and fixed on an elastic fabric base-④ to form the spring-like adaptive mechanism (Figure 3(a) III), which can follow the profile of the elbow to elongate or contract when the elbow flexes or extends (Figure 3(b)). To further reinforce the stiffness of the composite bellows, we refer to our previous work [30] and introduce the external con-

straints. Finally, inspired by Thalman's work [25], triangular retainers are fixed on both sides of the exosuit to enhance the force transmissibility between the exosuit and the elbow (Figure 3(a) IV).

Figure 3(c) illustrates the detailed principles of composite bellows and external constraints. When inflated, the exosuit inflects and produces torque dominated by the contact (i.e., interference) between the blades of the bellows. For exosuits with normal bellows (whether with or without adaptive mechanism), the effectiveness of contact is weak and limits the output force (Figure 3(c) I). The composite bellows with two branches in a blade can enhance the contact and improve the output force. However, only such composite bellows would topple with irregular deformation when deflated, making it difficult to actuate repetitively (Figure 3(c) II). The use of constraint can ensure the stability of each blade for repetitive actuation and increase the stiffness of composite bellows for higher output torque (Figure 3(c) III).

To reduce mechanical resistance, the elongation of the adaptive mechanism is required to match the profile elongation of the elbow. The geometric parameters must meet the following formula:

$$Nd\left(\frac{1}{\cos\alpha} - 1\right) = \Delta L_{\max}, \quad (2)$$

where the geometric parameters are: the number of blades of the composite bellows N , the original distance between the two blades d , the original inclined angle of the triangular pleats α . Other parameters include the height of the bellow h , the length of branches in blades of composite bellows l , and the width of the exosuit w (Figure 3(a)–(d)).

To verify our design, we specify these parameters on a health volunteer. The distance W of the volunteer is 30 mm, and the width of the exosuit w is 90 mm (comparable to the arm width of the volunteer). To achieve full ROM of the elbow flexion, set the maximum flexion angle of the joint $\theta_{\text{joint}}=\theta_{\text{max}}=130^\circ$ [29]. Other parameters are $N=8$, $h=40$ mm, $l=25$ mm, $\alpha=60^\circ$ and $\delta=15$ mm [31] to ensure a suitable size of the exosuit, and d can be obtained through eq. (2). Figure 3(e) shows the dimensions of the retainer and the constraint.

In this work, we compare three types of exosuits based on these structural features: exosuit with normal bellows (NB), exosuit with adaptive mechanism and normal bellows (AMNB), and exosuit with adaptive mechanism and composite bellows (AMCB). Apart from the structural features, the geometric parameters are set to be the same for each type of exosuit.

3 Fabrication and characterization

3.1 Fabrication

Figure 4 illustrates the primary fabrication process of the exosuit with AMCB as an example (see Supporting In-

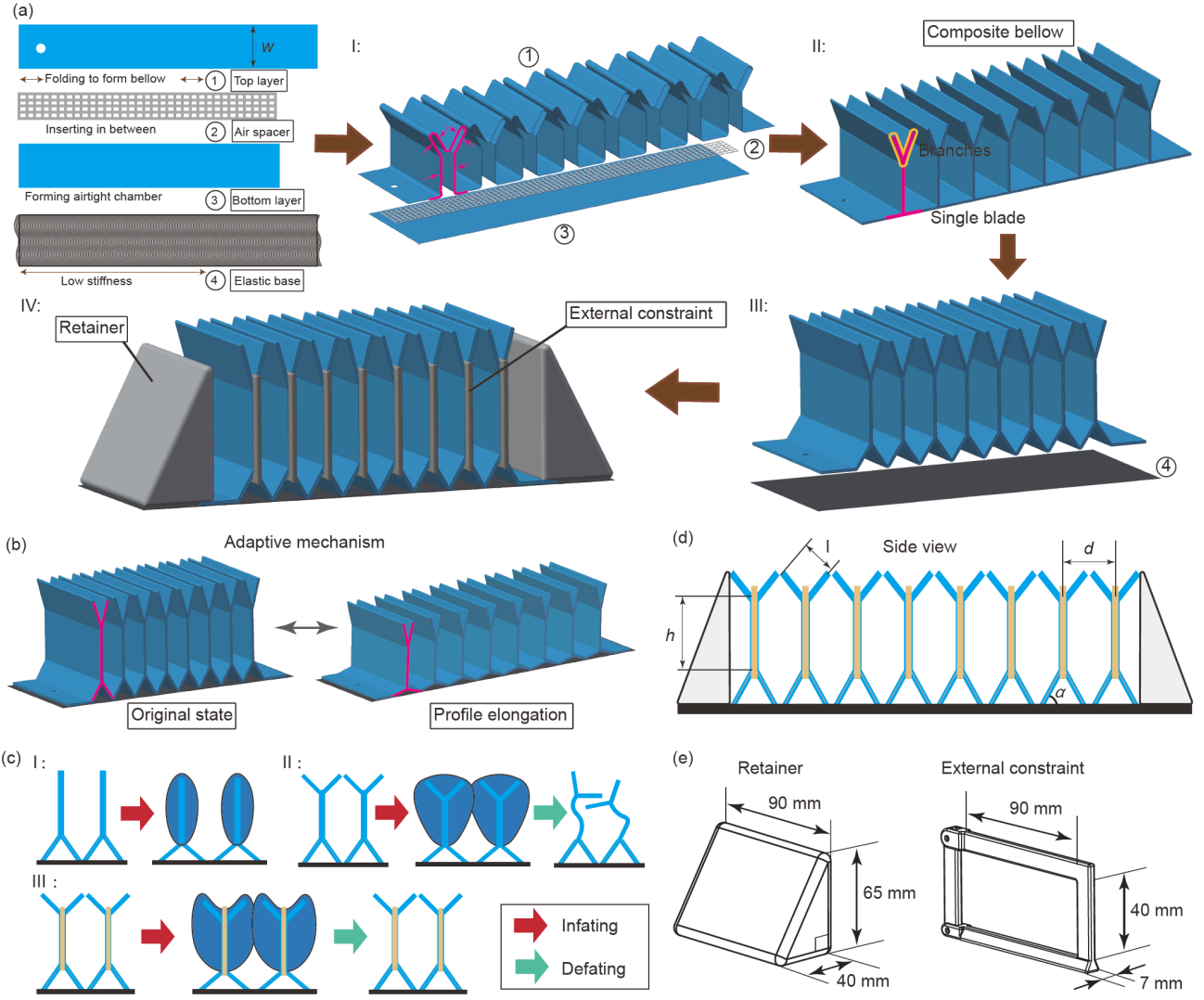


Figure 3 (Color online) The schematic structure and design principles of AMCB. (a) The schematic structure of AMCB; (b) demonstration of the adaptive mechanism that fits the elbow profile elongation; (c) demonstration of the detailed principles of introducing composite bellows and external constraint; (d) the geometric parameters to be determined in the ACMB; (e) the dimensions of a retainer and external constraint.

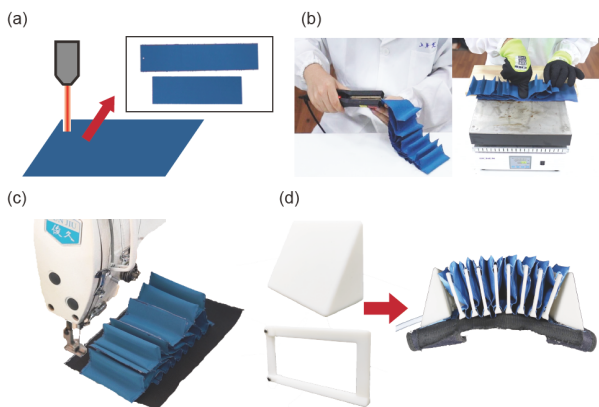


Figure 4 (Color online) The main fabrication process of AMCB. (a) Trim the textiles by laser cutting; (b) heat-seal the edges & bottom; (c) sew the base & sleeve; (d) assemble the constraints & retainers.

formation Movie S1).

(1) Use the laser cutter (VLS 3.50, Universal Laser Systems) to trim 3D rib weft-knitted polyester fabric coated with 0.2 mm-TPU into CAD patterns (Figure 4(a))

(2) Fold and heat-seal (180°C–200°C) the top layer to form branches in blades of composite bellows by using a thermal weld machine (FR-400 A, Blueberry). Then use a thermal welding plate (DB-XAB, LiChenKeYi) to heat-seal (180°C–200°C) the top layer, air spacer, and bottom layer to form an airtight chamber, as shown in Figure 4(b).

(3) Corrugate the exosuit bottom into triangle pleats and sew it on an elastic fabric base with sleeves using the sewing machine (Shanghai Junjiu Sewing Equipment Co., Ltd.), as shown in Figure 4(c).

(4) Assemble the constraints by inserting them into the

space between triangular pleats and branches of the bellows. Attach the retainers (hollow-carved with 2 mm wall thickness) with glue (cyanoacrylate adhesive, Xunlei). The constraints and retainers are manufactured with commercial 3D printing material (DSM IM-AGE8000, WeNext Technology Co., Ltd.) as shown in Figure 4(d).

3.2 Characterization

We characterize and compare the mechanical performance, including the mechanical resistance and output torque of NB (210.0 g), AMNB (217.2 g), and AMCB (344.2 g). For a fair comparison, the geometric parameters of the exosuits are controlled identically to each other except for the structural features.

Firstly, we measure the mechanical resistance during flexion. We set up a test rig composed of a torque sensor (TFF400, FUTEK) and a precision rotation guide (RSP 125-L, Dongguan Shengling Precision Machinery) with two adjacent-pleat plates to fix the exosuits for measurement. The rotation guide adjusts the joint angle between the plates for

different flexion states (Figure 5(a)). Meanwhile, we employ a 30 mm thick jig on the lateral side of plates, which simulates the structure of the elbow and produces profile elongation during flexion (i.e., when θ increases). The mechanical resistance of the exosuits is measured when the exosuit is deflated. To ensure the accuracy of the measurements, we slowly rotate the guide from 0° to 120° to maintain a quasi-equilibrium motion while simultaneously recording the resistance torque and corresponding rotation angle. For each type of exosuit, we repeat the measurement five times to reduce the impact of the random error.

Then, we characterize the output torque using the test rig mentioned above, a dSPACE (MicroLab Box, dSPACE) and a customized air control system (Deli Group Co., Ltd.) are used to supply compressed air at the required pressures. We measure the output torque at 0° , 60° , and 120° . For each joint angle, the supplied air pressure varies from 0 to 50 kPa with a step of 5 kPa. Likewise, we repeat the measurement five times to reduce the impact of the random error.

The experimental results of mechanical resistance are shown in Figure 5(a). The mechanical resistance of AMCB

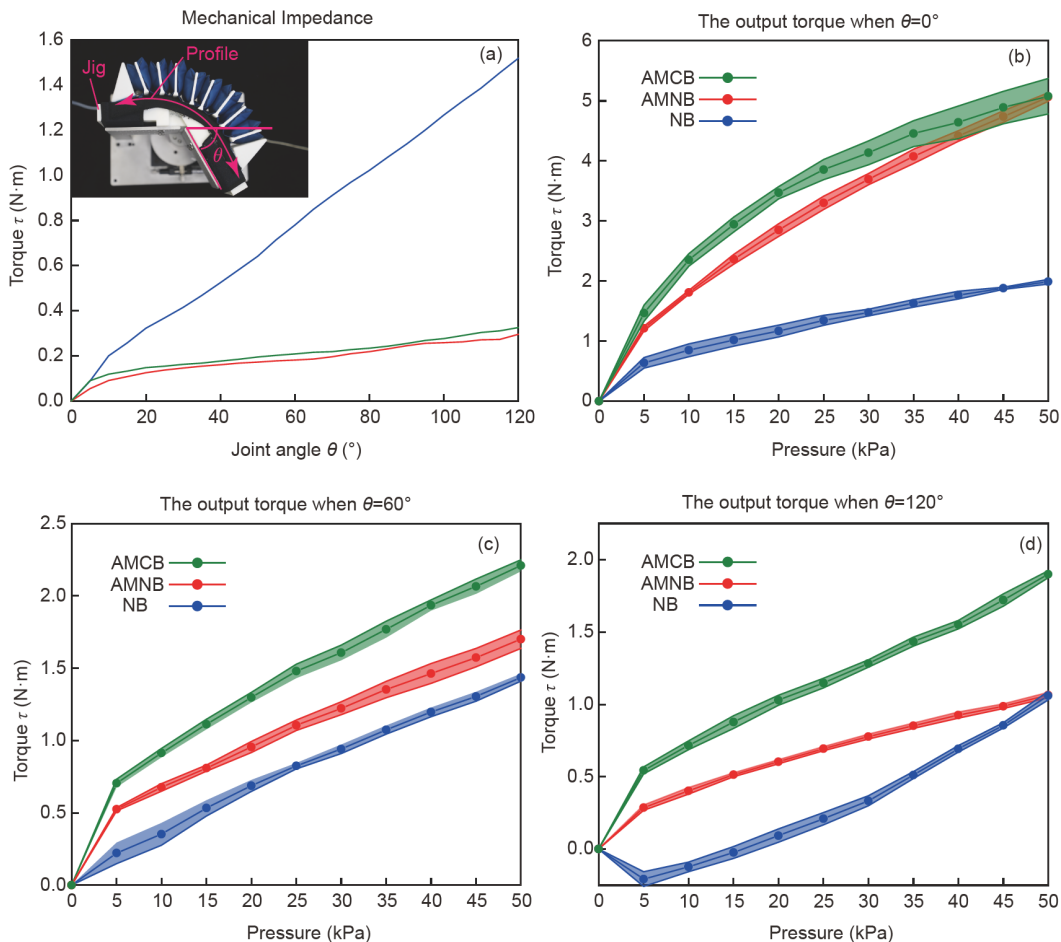


Figure 5 (Color online) The experimental results of mechanical resistance and output torque for three different kinds of elbow exosuit (NB, AMNB, AMCB). (a) The top view of the test rig for characterization and the mechanical resistance over the whole ROM; (b)–(d) the mean torque output (SD) at the joint angles of 0° , 60° , and 120° , respectively.

and AMNB is markedly lower than that of NB for the full range of the ROM. At the joint angle of 120° , the mechanical resistance is reduced by 80.6% (AMNB) and 78.6% (AMCB), proving the effectiveness of the adaptive mechanism.

The experimental results of output torque are shown in Figure 5(b)–(d). At all the measured joint angles, AMCB and AMNB have higher output torque than NB for the full range of the ROM. When $\theta=120^\circ$, the output torque is improved to 120.3% (AMNB) and 207.0% (AMCB) at 50 kPa, verifying the ability of the adaptive mechanism and the composite bellows to enhance the output force. The relationship between output torque and supplied pressure of the exosuit does not appear linear, which is inconsistent with the model built by relevant work [25,32] and may be caused by the geometric nonlinearity due to the large-scale elongation of the bottom layer and complicated contact between the bellows. Meanwhile, negative output torque by NB can be ob-

served at the joint angle of 120° when supplied pressure ranges from 0 to 15 kPa, which may ascribe to the mechanical resistance exceeding the active torque generated by the exosuit.

4 Experimental verification

4.1 Verification on wooden arm model

A wooden arm model is used to verify the assistance ability of the exosuits (see Supporting Information Movie S1). As shown in Figure 6(a), the wooden arm model (1.25 kg) comprises the upper arm and forearm, whose length and mass are 0.28 m, 0.55 kg and 0.46 m, 0.70 kg, respectively. The free ROM of the arm model is 0° – 130° , which is identical to the ROM of the human elbow. In the experiment, we wear the exosuit on the model and vertically fix the end of the upper arm. Next, we linearly pressurize the exosuit from

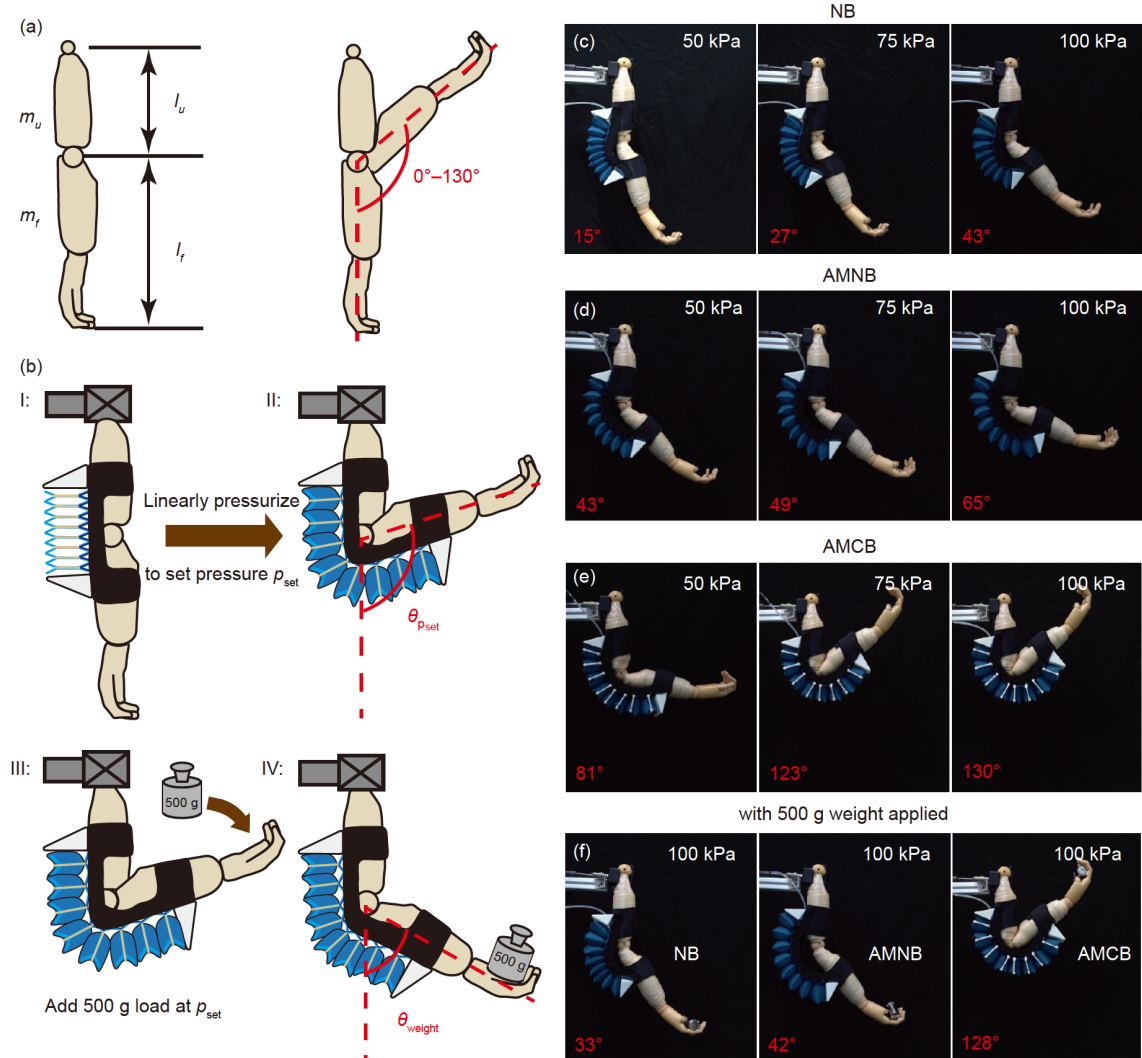


Figure 6 (Color online) Illustration and results of arm model test. (a) Components of the wooden arm model and its free ROM; (b) illustration of the testing process; (c)–(e) the ROM of the exosuits when the set pressure is 50, 75, and 100 kPa, respectively; (f) the lift capacity of the exosuits with 500 g weight.

0 kPa to the set pressure p_{set} . The corresponding joint angle at p_{set} is recorded as $\theta_{p_{\text{set}}}$ (Figure 6(b) I and II). Then, we maintain the pressure and apply 500 g weight onto the model. After equilibrium, the corresponding joint angle is recorded as θ_{weight} (Figure 6(b) III and IV).

The experimental results are shown in Figure 6(c)–(f). NB can hardly assist in flexion and lifting even under high pressure. As for AMNB, although the introduction of the adaptive mechanism improves the ROM, it still performs poorly in lifting weight. AMCB performs well in both ROM and lifting the weight, capable of covering the full ROM of 0°–130° and sustaining the weight at 100 kPa.

Moreover, with two ends of the exosuit fixed to the arm and the middle part remaining free, the exosuit might bulge outwards from the elbow if its output torque is not enough to lift the arm. The bulge is unfavorable to the realization of assistance capability and could be frequently observed on NB and AMNB. By comparison, AMCB provides enhanced output torque and can largely reduce the impact of this phenomenon, validating the effectiveness of our design.

4.2 Verification on health volunteer

We further verify the assistance ability of the exosuits through a health volunteer experiment (see Supporting In-

formation Movie S1). As shown in Figure 1, we integrate a wearable system composed of the elbow exosuit and belt package (including the controller, 958.5 g) remotely controlled by a smartphone. The controller is composed of an air pump (NMP 850.1.2 KPDC-B HP, KNF Technology Co., Ltd), a solenoid valve (xValve, Parker), a bluetooth (HC-06, Qi Xing Chong), an Arduino Nano (ATMEGA328, Arduino), and a lithium battery (NICJOY 24 V 2800 mAh, Nanjing Naizhuo Electronic Trading Co., Ltd). A flexible air tube is used to connect the elbow exosuit and the controller.

As shown in Figure 7(a), the health volunteer wears the exosuit on the right elbow and controls the system via the smartphone using the left hand. A 500 g weight is taped on the volunteer's wrist to avoid active muscle activities caused by grasping the weight. The volunteer is required to lift the weight over 90° in this experiment, where the surface electro-myographic (sEMG), as a metric of active muscle activity, is monitored through a pair of electrodes attached to the skin locations corresponding to the biceps and triceps, respectively (Trigno Wireless sEMG system, DEL-SYS INC.). Two working conditions in the lifting test are executed: with exosuit but no supplied pressure (pressure OFF), and with pressurized exosuit (pressure ON).

The sEMG activity of the biceps and triceps during lifting is shown in Figure 7(c), which is normalized to the maximum

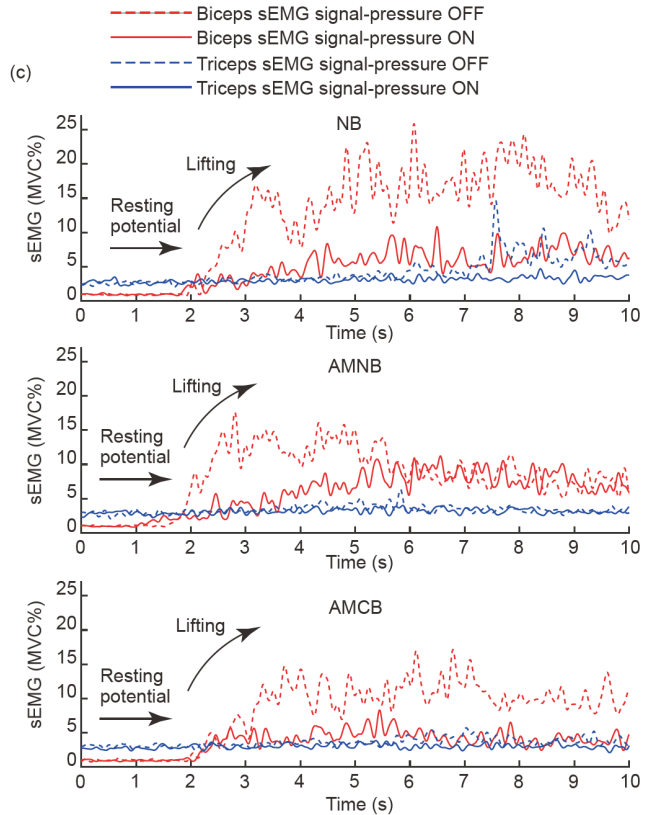


Figure 7 (Color online) Illustration and results of health volunteer experiment. (a) The experimental configuration of the health volunteer experiment; (b) the distribution of sEMG electrodes on the skin; (c) the sEMG activity of biceps and triceps when lifting 500 g weight.

voluntary contraction (MVC) of the volunteer [25,30]. In the case of pressure OFF, the sEMG activity of biceps and triceps with AMNB and AMCB is markedly lower than that with NB, demonstrating that the introduction of the adaptive mechanism reduces the mechanical resistance. In the case of pressure ON, all three exosuits can reduce the sEMG activity of the biceps and triceps, but AMCB keeps it at the lowest level, showing an improvement in assistance ability.

5 Conclusions

To address the challenges of remarkable mechanical resistance, small output force, and limited range of motion existing in current pneumatic soft elbow exosuits, we develop the fabric-based soft elbow exosuit with adaptive mechanism and composite bellows (AMCB) following elbow kinesiology. Compared with the exosuit with normal bellows (NB), AMCB can adapt to the profile of the elbow to elongate or contract when the elbow flexes or extends, achieving low mechanical resistance. In addition, the composite bellows, together with the external constraints, reinforce the exosuit stiffness and improves the output force. Characterization results show that with NB as the baseline, the mechanical resistance is significantly reduced by 78.6%, and the output torque is improved to 207.0% at 50 kPa for AMCB. The verification experiment on the arm model shows that AMCB could cover the full ROM of 0°–130° at the elbow while sustaining 500 g weight. The improvement of assistance ability is also observed from the reduction of sEMG activity in the lifting task of the health volunteer experiment.

Future work includes the analytical modelling or simulation of these exosuits, optimization of the geometric parameters for better mechanical performance, the introduction of soft components to replace the rigid components such as retainers and external constraints, integrating extension actuators for bidirectional elbow motion assistance, and the functional verification on patients in clinical trials.

This work was supported by the National Natural Science Foundation of China (Grant Nos. 52025057 and 91948302) and the Science and Technology Commission of Shanghai Municipality (Grant No. 20550712100).

Supporting Information

The supporting information is available online at tech.scichina.com and link.springer.com. The supporting materials are published as submitted, without typesetting or editing. The responsibility for scientific accuracy and content remains entirely with the authors.

- 1 Feigin V L, Brainin M, Norrving B, et al. World stroke organization (WSO): Global stroke fact sheet 2022. *Int J Stroke*, 2022, 17: 18–29
- 2 Hatem S M, Saussez G, Della Faille M, et al. Rehabilitation of motor function after stroke: A multiple systematic review focused on techniques to stimulate upper extremity recovery. *Front Hum Neurosci*,

- 3 Levin M F, Selles R W, Verheul M H G, et al. Deficits in the coordination of agonist and antagonist muscles in stroke patients: Implications for normal motor control. *Brain Res*, 2000, 853: 352–369
- 4 Day J M, Lucado A M, Uhl T L. A comprehensive rehabilitation program for treating lateral elbow tendinopathy. *Int J Sports Phys Ther*, 2019, 14: 818–829
- 5 Hu X, Tong K Y, Song R, et al. Variation of muscle coactivation patterns in chronic stroke during robot-assisted elbow training. *Arch Phys Med Rehabil*, 2007, 88: 1022–1029
- 6 Hogan N, Krebs H I, Charnnarong J, et al. MIT-MANUS: A workstation for manual therapy and training I. In: Proceedings of the IEEE International Workshop on Robot and Human Communication (RO-MAN). Tokyo, 1992. 161–165
- 7 Nef T, Mihelj M, Riener R. ARMin: A robot for patient-cooperative arm therapy. *Med Bio Eng Comput*, 2007, 45: 887–900
- 8 Perry J C, Rosen J, Burns S. Upper-limb powered exoskeleton design. *IEEE ASME Trans Mechatron*, 2007, 12: 408–417
- 9 Cianchetti M, Laschi C, Menciassi A, et al. Biomedical applications of soft robotics. *Nat Rev Mater*, 2018, 3: 143–153
- 10 Zhang J, Sheng J, O'Neill C T, et al. Robotic artificial muscles: Current progress and future perspectives. *IEEE Trans Robot*, 2019, 35: 761–781
- 11 Cappello L, Dinh Khanh B, Shih-Cheng Y, et al. Design and preliminary characterization of a soft wearable exoskeleton for upper limb. In: Proceedings of the IEEE International Conference on Biomedical Robotics and Biomechatronics (BioRob). Singapore, 2016. 623–630
- 12 Koo I, Yun C, Costa M V O, et al. Development of a meal assistive exoskeleton made of soft materials for polymyositis patients. In: Proceedings of the IEEE/RSJ International Conference on Intelligent Robots and Systems (IROS). Chicago, 2014. 542–547
- 13 Lessard S, Pansodtee P, Robbins A, et al. CRUX: A compliant robotic upper-extremity exosuit for lightweight, portable, multi-joint muscular augmentation. In: Proceedings of the International Conference on Rehabilitation Robotics (ICORR). London, 2017. 1633–1638
- 14 Noritsugu T, Takaiwa M, Sasaki D. Power assist wear driven with pneumatic rubber artificial muscles. In: Proceedings of the International Conference on Mechatronics and Machine Vision in Practice (M2VIP). Auckland, 2008. 539–544
- 15 Gao X F, Sun Y, Hao L, et al. A new type of soft pneumatic elbow. In: Proceedings of the IEEE International Conference on Robotics and Biomimetics (ROBIO). Macao, 2017. 2681–2686
- 16 Wilkening A, Stöppler H, Ivlev O. Adaptive assistive control of a soft elbow trainer with self-alignment using pneumatic bending joint. In: Proceedings of the IEEE International Conference on Rehabilitation Robotics (ICORR). Singapore, 2015. 729–734
- 17 Polygerinos P, Correll N, Morin S A, et al. Soft robotics: Review of fluid-driven intrinsically soft devices; manufacturing, sensing, control, and applications in human-robot interaction. *Adv Eng Mater*, 2017, 19: 1700016
- 18 Morris M, Shoham M, Nahon M, Applications and theoretical issues of cable-driven robots. In: Proceedings of the Florida Conference on Recent Advances in Robotics (FCRAR). Florida, 2009. 21–22
- 19 Park D, Cho K J. Development and evaluation of a soft wearable weight support device for reducing muscle fatigue on shoulder. *PLoS ONE*, 2017, 12: e0173730
- 20 Bessler J, Prange-Lasonder G B, Schaake L, et al. Safety assessment of rehabilitation robots: A review identifying safety skills and current knowledge gaps. *Front Robot AI*, 2021, 8: 602878
- 21 Sanchez V, Walsh C J, Wood R J. Textile technology for soft robotic and autonomous garments. *Adv Funct Mater*, 2021, 31: 2008278
- 22 O'Neill C T, Phipps N S, Cappello L, et al. A soft wearable robot for the shoulder: Design, characterization, and preliminary testing. In: Proceedings of the International Conference on Rehabilitation Robotics (ICORR). London, 2017. 1672–1678
- 23 Koh T H, Cheng N, Yap H K, et al. Design of a soft robotic elbow sleeve with passive and intent-controlled actuation. *Front Neurosci*,

- 2017, 11: 597
- 24 Proietti T, O'Neill C, Hohimer C J, et al. Sensing and control of a multi-joint soft wearable robot for upper-limb assistance and rehabilitation. *IEEE Robot Autom Lett*, 2021, 6: 2381–2388
- 25 Thalman C M, Lam Q P, Nguyen P H, et al. A novel soft elbow exosuit to supplement bicep lifting capacity. In: Proceedings of the IEEE/RSJ International Conference on Intelligent Robots and Systems (IROS). Madrid, 2018. 6965–6971
- 26 Miller-Jackson T M, Li J, Natividad R F, et al. STAS: An antagonistic soft pneumatic actuator assembly for high torque output. In: Proceedings of the IEEE International Conference on Soft Robotics (RoboSoft). Seoul, 2019. 43–48
- 27 Nassour J, Vaghani S, Hamker F H. Design of soft exosuit for elbow assistance using butyl rubber tubes and textile. In: Proceedings of the International Symposium on Wearable Robotics (WeRob). Pisa, 2018.
- 420–424
- 28 Nassour J, Zhao G, Grimmer M. Soft pneumatic elbow exoskeleton reduces the muscle activity, metabolic cost and fatigue during holding and carrying of loads. *Sci Rep*, 2021, 11: 1–4
- 29 Neumann D A. Kinesiology of the Musculoskeletal System: Foundations for Rehabilitation. 2nd ed. Mosby: Elsevier, 2010
- 30 Feng M, Yang D, Gu G. High-force fabric-based pneumatic actuators with asymmetric chambers and interference-reinforced structure for soft wearable assistive gloves. *IEEE Robot Autom Lett*, 2021, 6: 3105–3111
- 31 Schuind F A, Goldschmidt D, Bastin C, et al. A biomechanical study of the ulnar nerve at the elbow. *J Hand Surg*, 1995, 20: 623–627
- 32 Park J, Choi J, Kim S J, et al. Design of an inflatable wrinkle actuator with fast inflation/deflation responses for wearable suits. *IEEE Robot Autom Lett*, 2020, 5: 3799–3805